nature genetics

PNPLA1 mutations cause autosomal recessive congenital ichthyosis in golden retriever dogs and humans

Anaïs Grall[1,2], Eric Guaguère[3], Sandrine Planchais[1,2], Susanne Grond[4], Emmanuelle Bourrat[5], Ingrid Hausser[6,7], Christophe Hitte[1,2], Matthieu Le Gallo[1,2], Céline Derbois[8], Gwang-Jin Kim[9,10], Laëtitia Lagoutte[1,2], Frédérique Degorce-Rubiales[11], Franz P W Radner[4], Anne Thomas[12], Sébastien Küry[1,2,13], Emmanuel Bensignor[14], Jacques Fontaine[15], Didier Pin[16], Robert Zimmermann[4], Rudolf Zechner[4], Mark Lathrop[8,17], Francis Galibert[1,2], Catherine André[1,2,19] & Judith Fischer[8,9,18,19]

© 2012 Nature America, Inc. All rights reserved.

Ichthyoses comprise a heterogeneous group of genodermatoses characterized by abnormal desquamation over the whole body, for which the genetic causes of several human forms remain unknown. We used a spontaneous dog model in the golden retriever breed, which is affected by a lamellar ichthyosis resembling human autosomal recessive congenital ichthyoses (ARCI), to carry out a genome-wide association study. We identified a homozygous insertion-deletion (indel) mutation in *PNPLA1* that leads to a premature stop codon in all affected golden retriever dogs. We subsequently found one missense and one nonsense mutation in the catalytic domain of human *PNPLA1* in six individuals with ARCI from two families. Further experiments highlighted the importance of PNPLA1 in the formation of the epidermal lipid barrier. This study identifies a new gene involved in human ichthyoses and provides insights into the localization and function of this yet uncharacterized member of the PNPLA protein family.

Ichthyoses in humans encompass a heterogeneous group of hereditary cornification disorders with generalized scaling of the skin due to defects in terminal differentiation of keratinocytes and desquamation, which occur in the upper layer of the epidermis. Whereas autosomal ichthyosis vulgaris is a common, mild disease, other forms are mostly rare, congenital diseases, such as ARCI, including the very severe harlequin ichthyosis[1]. The molecular mechanisms identified to date are related to skin barrier function defects, involving three major components of the epidermal barrier: the intercellular lipid barrier, the cornified cell envelope and keratin or filaggrin degradation products. In addition to these nonsyndromic forms, several ichthyosiform phenotypes are classified as syndromic ichthyoses (for example, Netherton syndrome, Chanarin-Dorfman syndrome, Refsum's disease and Sjögren-Larsson syndrome)[1].

In humans, positional cloning and homozygosity mapping of families with ARCI have highlighted several loci and causative genes[2]. To date, around 40 genes involved in either syndromic or nonsyndromic ichthyoses have been described[1]. However, mutations in these genes do not explain all the clinical forms of ichthyosis. In our collection of individuals and families presenting with ARCI, the molecular cause has been determined for 80% of the affected individuals. Causative mutations have been identified in seven genes: *TGM1*, *ALOX12B*, *ALOXE3*, *ABCA12*, *NIPAL4* (ichthyin), *CYP4F22* (ref. 2) and *LIPN*[3].

Chanarin-Dorfman syndrome (OMIM 275630), defined as neutral lipid storage disease with ichthyosis (NLSDI), is a syndromic ichthyosis associated mainly with a mild myopathy and hepatomegaly and has been shown to be caused by mutations in *ABHD5* (also known as *CGI-58*)[4]. This discovery highlighted the major role of lipid metabolism in keratinization and formation of the skin barrier[5]. Indeed, CGI-58, initially described as an esterase/lipase/thioesterase protein, acts as an activator of adipose triglyceride lipase (ATGL; also known as patatin-like phospholipase domain-containing protein 2 (PNPLA2)) and promotes the PNPLA2-dependant hydrolysis of triglycerides into free fatty acids and diacylglycerols[6–8]. In fact, *PNPLA2* mutations have been found to be responsible for neutral lipid storage disease with myopathy (NLSDM). Affected individuals develop hepatomegaly, severe myopathy and cardiac abnormalities but no ichthyosis[9,10].

[1]Centre National de la Recherche Scientifique (CNRS), Institut de Génétique et Développement de Rennes, Rennes, France. [2]Université Rennes 1, Institut Fédératif de Recherche (IFR) 140, Faculté de Médecine, Rennes, France. [3]Clinique Vétérinaire Saint Bernard, Lomme, France. [4]Institute of Molecular Biosciences, Karl-Franzens-Universität Graz, Graz, Austria. [5]Département de Dermatologie, Hôpital St. Louis, Paris, France. [6]Department of Dermatology, University Clinic Heidelberg, Heidelberg, Germany. [7]Electron Microscopy Core Facility University Heidelberg, Heidelberg, Germany. [8]Institut de Génomique, Centre National de Génotypage (CNG), Commissariat à l'Enérgie Atomique et aux Enérgies Alternatives (CEA), Evry, France. [9]Institute for Human Genetics, University Clinic Freiburg, Freiburg, Germany. [10]Faculty for Biology, University of Freiburg, Freiburg, Germany. [11]Laboratoire d'Anatomie Pathologique Vétérinaire du Sud-Ouest, Toulouse, France. [12]Antagene, Animal Genetics Laboratory, Limonest, France. [13]Centre Hospitalier Universitaire (CHU) Nantes, Service de Génétique Médicale, Nantes, France. [14]Clinique Vétérinaire de la Boulais, Cesson-Sévigné, France. [15]Clinique Vétérinaire, Brussels, Belgium. [16]Unité de Dermatologie, VetAgro Sup Campus Vétérinaire de Lyon, Marcy l'Etoile, France. [17]Fondation Jean Dausset–Centre d'Etude de Polymorphisme Humain (CEPH), Paris, France. [18]Zentrum für Biosystemanalyse, Universität Freiburg, Freiburg, Germany. [19]These authors jointly directed this work. Correspondence should be addressed to C.A. (catherine.andre@univ-rennes1.fr) or J. Fischer (judith.fischer@uniklinik-freiburg.de).

Received 4 May 2011; accepted 5 December 2011; published online 15 January 2012; doi:10.1038/ng.1056

Mutations in *PNPLA2* have been found in sequences encoding the patatin domain[11] and at the 3′ end of the gene[9]. Defects in the hydrophobic domain lead to a block in triglyceride degradation[8], thus inducing a systemic accumulation of triglycerides into cytoplasmic droplets in many cell types, including leukocytes from peripheral blood smears[6].

The PNPLA protein family contains nine members characterized by the presence of a highly conserved patatin domain[12,13]. PNPLA family members have diverse lipolytic and acyltransferase activities and are key elements in lipid metabolism[14,15]. They are divided into three subfamilies: a group containing PNPLA1 to PNPLA5, another containing the neuropathy target esterases (PNPLA6 and PNPLA7) and the last group, which are phospholipases and include the calcium-independent phospholipase A_2 proteins (PNPLA8 and PNPLA9). Four of these enzymes have already been implicated in human diseases: PNPLA2 (ref. 9), PNPLA3 (refs. 16,17), PNPLA6 (ref. 18) and PNPLA9 (refs. 19–21). The other five members have not yet been implicated in any disease.

In humans, identifying the genetic causes of rare diseases remains challenging because of the difficulties in collecting enough families affected by a unique clinical entity. Of the available genetic models, the dog seems relevant because each pure breed represents a group of genetically similar animals descended from only a few ancestors. Dog breeds have been artificially created by humans, and this selective breeding has resulted in the extreme phenotypic diversity exhibited across breeds. Inbreeding practices, aimed at selecting particular phenotypic or behavioral traits in each breed, led to the selection of alleles governing the desired phenotypes but also resulted in the selection of undesirable alleles[22,23]. These practices explain the large number of spontaneous breed-specific diseases reported in dogs[22,24]. Thus, the dog is a unique model for pinpointing phenotype-genotype correlations by analyzing cases and controls, either by examining a founder effect within a breed by searching for the smallest chromosomal region containing the variation or by analyzing fixed traits across breeds by searching for the smallest shared haplotypes[24–26]. These strategies include family-based genetic linkage approaches or genome-wide association studies (GWAS) with a limited number of dogs in one or several breeds[23,27].

In dogs, a dozen breed-specific ichthyoses have been clinically described, but the molecular mechanisms are not all understood because the responsible genes have been identified in only two breeds. The Norfolk terrier breed presents a mild recessive epidermolytic hyperkeratosis caused by a splice-site mutation in the *KRT10* (Keratin 10) gene[28]. The Jack Russell terrier breed presents a severe nonepidermolytic ichthyosis, for which a LINE-1 insertion in the *TGM1* gene has been recently identified[29]. The causative genes implicated in these two breeds have already been described in humans, and, therefore, these dogs constitute relevant therapeutic models for their human counterparts[1,30–33].

In golden retrievers, a hereditary nonepidermolytic retention ichthyosis was diagnosed and described for the first time in 2007 (refs. 34,35). More recently, the clinical, epidemiological and histopathological characteristics of this disease have been precisely analyzed, and an autosomal recessive transmission mode has been proposed[36–38]. Dermatological signs, visible at as early as a few weeks of age, include a mild, moderate or severe generalized scaling, initially with small to large whitish scales and progressively with blackish scales.

Here, in a genetic association study using only 40 golden retriever dogs, we identified a single locus that shows highly significant association and found a mutation in the *PNPLA1* gene (Gene ID 481763) that perfectly segregates with the disease. Based on the information obtained from the dog genetic model, we identified mutations in the *PNPLA1* gene (Gene ID 285848) in two unrelated human families with ARCI for which no causative gene had been identified to date. Besides enabling the identification of a new gene causing a rare form of human ichthyosis, this work provides knowledge about the expression and function of PNPLA1, an as yet uncharacterized protein involved in lipid metabolism in the cutaneous barrier.

RESULTS

Identification of a *PNPLA1* mutation in dogs

We performed a GWAS using the Affymetrix v2 canine SNP array with 40 golden retriever dogs (20 affected dogs (cases) and 20 controls) and identified an associated genomic region of 8.1 Mb (between positions 3.9 and 12 Mb) on canine chromosome 12 (*Canis familiaris* chromosome, CFA12) comprising 217 annotated genes. The most significant *P* values defining the critical interval were determined with PLINK software[39] ($P_{raw} \leq 2.1 \times 10^{-7}$; *P* value after Bonferroni correction $\leq 3.8 \times 10^{-3}$). A shared region of homozygosity spanning 8.55 to 9.66 Mb was observed in all affected dogs and was never observed in control dogs, reducing the interval to 1.1 Mb. This region of homozygosity contains 21 annotated genes, including the patatin-like phospholipase domain-containing protein 1 gene *PNPLA1*, which is a paralog of *PNPLA2*. We considered *PNPLA1* to be a promising candidate gene, as *PNPLA2* is regulated by CGI-58, the gene product disrupted in NLSDI (Chanarin-Dorfman syndrome)[4].

PNPLA1 has not previously been reported to be involved in any genodermatosis or in any other lipid metabolism defect. This gene is poorly characterized, with only a genomic sequence deduced by sequence comparisons, and neither its expression nor the function of its product has been described[12–15]. Of the 40 golden retriever dogs analyzed in the GWAS, we carried out mutation screening in 12 cases and 12 controls. Sequencing of the 10 exons and all the exon-intron boundaries of *PNPLA1* identified an indel in exon 8 in all 12 of the affected dogs analyzed (**Fig. 1**). The indel consists of a 3-bp

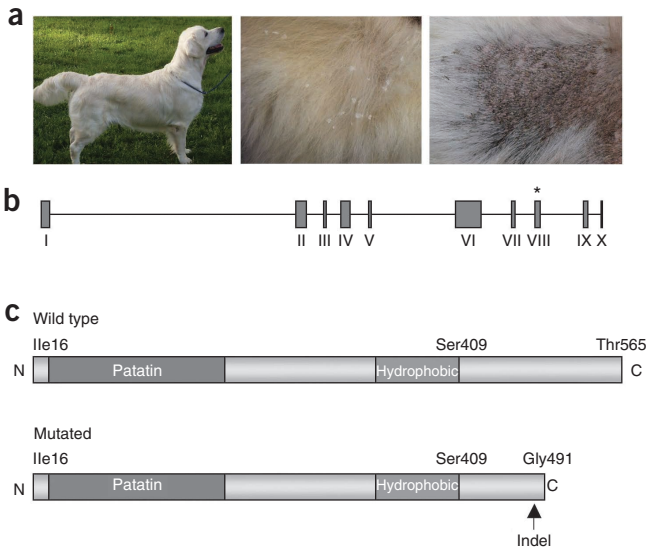

Figure 1 Identification of the *PNPLA1* mutation in affected golden retriever dogs. (**a**) In these dogs, generalized scaling, with white or blackish scales, and large ichthyosiform adherent scales are suggestive of ichthyosis. (**b**) The structure of the dog *PNPLA1* gene. Sequencing *PNPLA1* in affected dogs revealed an indel in exon 8 indicated by a star. (**c**) Predicted structure of wild-type and mutant PNPLA1 proteins, including the patatin domain (beginning at Ile16) and hydrophobic domain (ending at Ser409). The mutation induces a frameshift and a premature stop codon. International patent for the detection of the mutation in dogs: PCT/EP2010/067569.

© 2012 Nature America, Inc. All rights reserved.

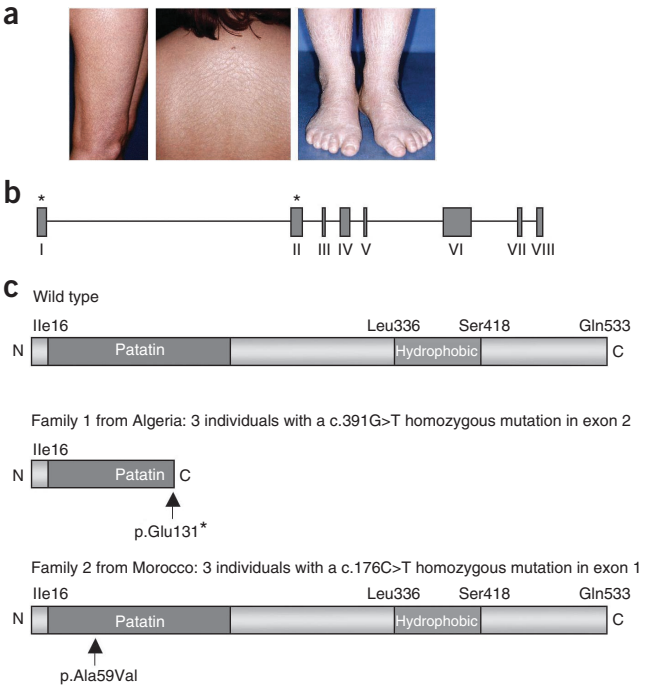

Figure 2 Identification of *PNPLA1* mutations in humans with autosomal recessive congenital ichthyosis. (**a**) Clinical example of ARCI. Two affected sisters (35 and 37 years of age) from the consanguineous Algerian family, born as collodion babies, present similar dermatological characteristics. While they are treated with emollients, the clinical features are the following: nonbullous and nonsyndromic congenital ichthyosiform erythroderma with diffuse mild erythema, mild hyperkeratosis with thin, white and adhesive scales, diffuse even in the flexures, with a reticulated aspect on the back and thighs. Hyperkeratosis is more severe with larger and octagonal scales on the legs. There is a mild palmo-plantar keratoderma, a pseudo-syndactyly of the second and third toes. The older sister has been treated since age 35 with acitretin (0.25 mg/kg/d) and keratolytic topics; her erythroderma is more pronounced but the scaling has totally disappeared across the integument (also see **Supplementary Fig. 3**). (**b**) The structure of the human *PNPLA1* gene and sites of the mutations (exon 1 and 2) indicated by the stars. (**c**) Predicted structure of wild-type and mutant PNPLA1 proteins, including the patatin domain (beginning at Ile16) and hydrophobic domain (between Leu336 and Ser418). In family 1, the nonsense mutation c.391G>T leads to a premature stop codon at position 131. In family 2, the missense mutation c.176C>T leads to a p.Ala59Val substitution. Informed consent was obtained from the individuals pictured here.

deletion followed by an 8-bp insertion, resulting in an insertion of 5 bp (**Supplementary Fig. 1**). We confirmed this result by sequencing a set of 320 golden retriever dogs with known clinical status (120 affected, 200 unaffected). All 120 affected dogs were homozygous for the mutation, and all 200 unaffected dogs were either homozygous for the wild-type allele or heterozygous (40% and 60%, respectively), which is concordant with an autosomal recessive transmission mode. The mutation was not detected in a panel of 180 healthy dogs belonging to the other four retriever breeds or in 300 healthy dogs from 25 different breeds. These data support the causative nature of the mutation in the golden retriever breed as well as the specific founder effect in this breed. The indel, resulting in an insertion of 5 bp, introduces a frameshift and, thus, a premature stop codon in the open reading frame of the gene, leading to the loss of 74 amino acids in the highly conserved C-terminal region of the PNPLA1 protein (**Fig. 1**).

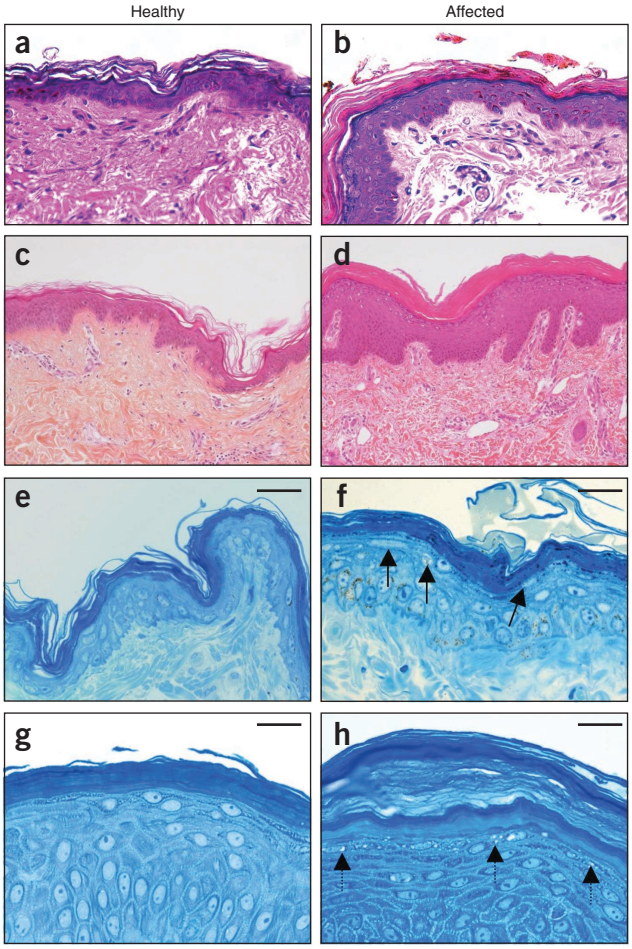

Figure 3 Histological analysis of skin biopsies from golden retriever dogs and human subjects. (**a**–**d**) Hematoxylin and eosin staining of skin biopsies from a healthy dog (**a**), a dog affected with ichthyosis (original magnification 400×) (**b**), a healthy human (**c**) or an individual with ARCI (original magnification 200×) (**d**). (**e**–**h**) Light microscopy images of semi-thin sections of skin biopsies stained with methylene blue from a healthy dog (**e**), a dog affected with ichthyosis (**f**), a healthy human (**g**) or an individual with ARCI (**h**). Biopsies of affected individuals are characterized by a pronounced hyperkeratosis with a homogenous thicker compact orthokeratotic cornified layer as well as a thicker granular layer. Black arrows in **f** indicate vacuolic structures in keratinocytes from the subgranular layer of affected dog biopsies. Black dotted arrows in **h** indicate small holes within granular layer of human biopsies. Scale bars, 20 μm.

Identification of *PNPLA1* mutations in humans

To study the involvement of this gene in human ichthyoses, we selected individuals from a cohort of 46 consanguineous families with ARCI that had undergone genome-wide linkage analyses with both SNPs and microsatellites and in which no causative mutation had been found in genes known to have a role in ARCI (**Supplementary Note**). We selected ten families in which the affected individuals showed a homozygous haplotype in the 6p21 region containing the human *PNPLA1* gene (orthologous to position 8.55 to 9.66 Mb on canine chromosome 12). Sequencing identified two distinct mutations in two of the ten families. In the first family, from Algeria, the three affected individuals had a homozygous nonsense mutation in exon 2 of *PNPLA1* (isoform 1), which resulted in a G to T transversion in the cDNA at position 391 downstream of the start codon (c.391G>T). This mutation introduces a premature stop codon at position 131 within the patatin domain, leading to a severely truncated protein

© 2012 Nature America, Inc. All rights reserved.

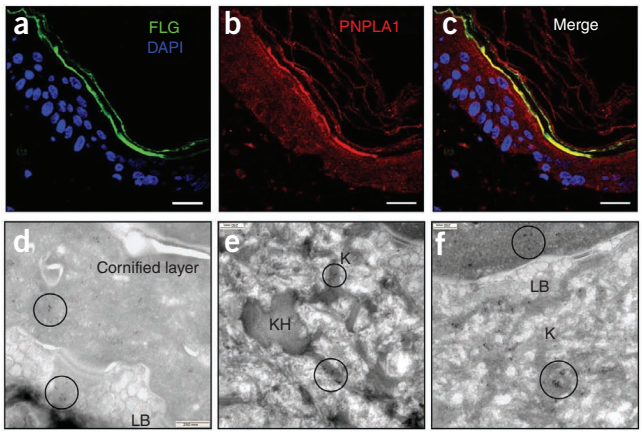

Figure 4 Localization of wild-type PNPLA1 protein in human skin. (**a**–**c**) Confocal microscopy images of double immunostained human skin paraffin section from a healthy individual for the granular layer marker FLG (filaggrin); green) with DAPI as nuclear counterstaining (blue) (**a**) and PNPLA1 (red), indicating its expression throughout the epidermis (**b**). (**c**) The merged image shows colocalization of the two proteins, suggesting coexpression of PNPLA1 in the granular layer together with filaggrin. Scale bars, 20 μm. (**d**–**f**) Immunoelectron microscopy observations of the PNPLA1 protein in cryo-ultrasection from a healthy individual showing labeling in the regions of keratin filament bundles, predominantly in the upper epidermal layer (as shown by circles). K, keratin filament bundles; KH, keratohyalin; LB, lamellar bodies. Scale bars, 250 nm.

(p.Glu131*). The mutation in this family segregated in an autosomal recessive manner: both parents and three available siblings, all unaffected, were heterozygous for the mutation. In the second family, from Morocco, the three affected children carried a homozygous missense mutation in exon 1, which replaced an alanine residue with valine at amino acid position 59 (isoform 1: c.176C>T (GCC>GTC), p.Ala59Val). Both parents and two unaffected siblings were heterozygous for this mutation (**Fig. 2**). The functional effect of this variant was evaluated using PolyPhen-2 v2 (ref. 40) with a result score of 1.0, indicating a probable damaging mutation. In addition, this altered amino acid is located in the patatin domain of the PNPLA1 protein and is conserved in several species (**Supplementary Fig. 2**). No *PNPLA1* mutations were detected in a panel of 384 control DNA samples (North African and European). Notably, all six affected individuals were born as collodion babies, later having generalized ichthyosis with fine white scales and moderate erythroderma and palmoplantar keratoderma (**Supplementary Fig. 3** and **Supplementary Table 1**). Two of the affected individuals from the Algerian family were overweight and exhibited pseudosyndactyly of the second and third toes (**Fig. 2a**). Blood smear analysis did not show intracellular inclusions (lipid vacuoles) similar to those found in Chanarin-Dorfman syndrome[5].

PNPLA1 transcript expression and sequence in dogs

We determined the expression profile of *PNPLA1* in 23 different dog tissues by RT-PCR analysis. We observed strong expression in the skin, which is concordant with the involvement of the PNPLA1 protein in a genodermatosis, as well as weak expression in the occipital lobe of the brain and even less in the spinal cord and the colon (**Supplementary Fig. 4a**). Consistent with the expected function of PNPLA1 in skin, we found a systematic expression in total skin, lip, pad and nose. Moreover, we found that the *PNPLA1* transcript in skin is specifically expressed in keratinocytes and not in fibroblasts. Sequencing of *PNPLA1* cDNA showed that the mutation is present in the cDNA of affected and carrier dogs; the transcript sequence in the skin is shown in **Supplementary Figure 4b**. As expected, real-time PCR confirmed the allelic distribution of the wild-type and mutated alleles in affected, carrier and healthy dogs. Notably, we observed that the mutant *PNPLA1* mRNA was expressed at a lower level (50% less) in affected dogs compared with healthy dogs and carriers (**Supplementary Fig. 4c**).

Localization of PNPLA1 protein and morphological studies

Histopathology carried out on affected golden retriever dogs and one affected individual from family 1 showed compact orthokeratotic epidermal hyperkeratosis composed of many layers of completely keratinized epidermal cells and pronounced acanthosis in the epidermis (**Fig. 3**). Affected skin presented with a thicker cornified layer, pronounced desquamation of upper, loosely packed scales and hypergranulosis with increased amounts of keratohyalin. Cytoplasmic vacuolic structures (optically empty after hematoxylin and eosin (H&E) staining) were visible on semi-thin sections in keratinocytes from the subgranular layer in affected dogs, and conspicuous regularly spaced small holes were visible in the granular layer in the affected person's skin (**Fig. 3**).

Immunofluorescence performed using confocal microscopy on healthy human skin showed the presence of PNPLA1 in the epidermis. The colocalization of PNPLA1 and filaggrin suggests stronger expression of PNPLA1 in the granular layer (**Fig. 4a**–**c**). Immunohistochemistry experiments also showed staining of the upper epidermis and eccrine sweat gland cells of the dermis in healthy human skin (diaminobenzidine (DAB) staining, data not shown). Immunoelectron microscopy experiments showed labeling of PNPLA1 in the region of keratin filament bundles, which was more pronounced in upper epidermal layers and in the lower layers of the cornified layer. No labeling was detected in dermal extracellular matrix structures or in keratohyalin granules (**Fig. 4d**–**f**). Notably, lamellar bodies were not stained, suggesting that PNPLA1 is not present in these organelles, in contrast to CGI-58 (ref. 41). Together, these data are concordant with previous immunohistochemistry and immunofluorescence experiments reported in the Human Protein Atlas.

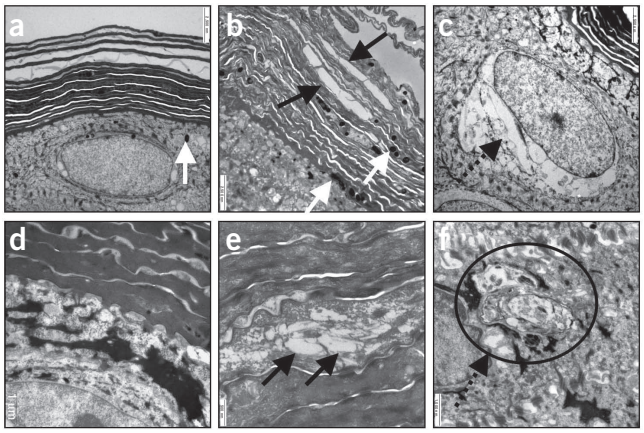

Figure 5 Transmission electron micrographs of fixed fresh skin biopsies from golden retriever dogs and humans. Electron microscopy of skin biopsies from (**a**) a healthy dog, (**b**,**c**) dogs affected with ichthyosis, (**d**) a healthy human or (**e**,**f**) individuals with ARCI. White arrows indicate pigment granules; black arrows indicate cholesterol clefts in the cornified layer in **b** and **e**; black dotted arrows indicate irregular accumulations of abnormal membranous and vesicular material around the nuclei of cells from the granular layer in **c** and **f**. Scale bars in **a**–**c**, 2.5 μm. Scale bars in **d** and **f**, 1 μm. Scale bar in **e**, 0.5 μm.

© 2012 Nature America, Inc. All rights reserved.

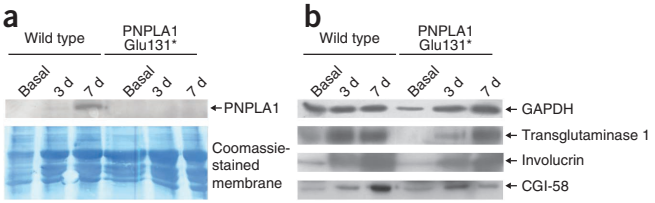

Figure 6 Protein blotting of PNPLA1 in normal and mutant human keratinocytes, before differentiation and at 3 and 7 d after induction of differentiation. (**a**) PNPLA1 protein was detected at ~58 kDa using antibody against PNPLA1. To confirm equal protein loading, membranes were stained with Coomassie blue. (**b**) Detection of proteins was performed using antibodies against transglutaminase 1, involucrin and CGI-58; GAPDH was used as a loading control. Transglutaminase 1 was detected at ~90 kDa, involucrin at ~120 kDa, CGI-58 at ~39 kDa and GAPDH at ~37 kDa.

Ultrastructural analyses were carried out on skin biopsies from six golden retrievers, of whom two were affected, and from two human individuals, of whom one was a healthy control and the other was an affected individual from family 1 (**Fig. 5**). In addition to a massive and compact orthohyperkeratosis, two main abnormalities were observed. First, in affected dogs, regular groups of electron-lucent polyclonal clefts were detected within lamellae of the cornified layer, corresponding to remnants of cholesterol crystals (**Fig. 5b**). Second, in keratinocytes of the granular layer, irregular accumulations of abnormal membranous and vesicular material were seen, suggesting a degenerative process of the intracellular membrane trafficking system (**Fig. 5c**). These areas correspond to the perinuclear vacuolic regions observed with H&E staining. Electron microscopy of the biopsy from the affected individual in family 1 showed more than 40 layers of cornified lamellae, consisting partly of loose content but otherwise mainly homogenous, with some lipid droplets, membrane structures and increased amounts of melanosomal remnants. There were only a few remnants of cholesterol crystals (**Fig. 5e**). In the transition to the living epidermal layers, there were many transit cells and numerous vesicular structures within the cells of the granular layer, corresponding to the holes observed in light microscopy. These vesicular structures were either optically empty or contained single or several small vesicles, melanosomal remnants or aberrant membranous structures (**Fig. 5f**). Occasionally, increased amounts of vesicular or membranous structures were deposited to the perinuclear region, similar to what was found in the skin of affected dogs.

Functional studies of wild-type and mutant PNPLA1 proteins

To gain insights into PNPLA1 function, we cultured wild-type and mutant keratinocytes from one affected individual from family 1 with a p.Glu131* mutation in PNPLA1. First, we analyzed PNPLA1 expression during *in vitro* differentiation of keratinocytes. PNPLA1 protein was not detected under basal conditions and increased during differentiation of wild-type keratinocytes. As expected, PNPLA1 was not detected in mutant keratinocytes, either at basal or at differentiated stages, indicating that PNPLA1 was not present in the affected individual's cells (**Fig. 6a**). Subsequently, we determined the differentiation capacity of cells by expression analysis of keratinocyte markers, such as involucrin, transglutaminase 1 (TGM1) and CGI-58. Involucrin is an early expressed component of the cornified envelope[42] and is crosslinked by TGM1, an enzyme mainly expressed in the granular layer[43]. Involucrin and TGM1 were strongly induced during differentiation, both in wild-type and mutant keratinocytes, suggesting that differentiation occurs independently of the presence of PNPLA1. CGI-58, which is predominantly expressed in cells in the granular layer where it localizes to lamellar granules[41], was present under basal conditions and showed increased expression after induction of differentiation in wild-type keratinocytes. Of note, upregulation of CGI-58 was not observed in mutant cells after 7 days of differentiation, indicating that PNPLA1 deficiency could affect the correct formation of lamellar bodies (**Fig. 6b**).

Since PNPLA1 has high homology with PNPLA2, a major triglyceride lipase in many cell types, we tested whether PNPLA1 deficiency affects the neutral lipid profile of keratinocytes. Wild-type and mutant keratinocytes were differentiated for 7 days, and lipids were then analyzed by thin-layer chromatography. The neutral lipid pattern of wild-type and PNPLA1-deficient keratinocytes did not show any detectable difference in triglyceride and cholesterol ester content, arguing against an involvement of PNPLA1 in neutral lipid catabolism (**Fig. 7a**). To further exclude a role for PNPLA1 in triglyceride catabolism, we tested whether PNPLA1 harbors triglyceride hydrolase activity in the presence or absence of CGI-58, the co-activator of PNPLA2. For this purpose, we expressed PNPLA1, PNPLA2 and CGI-58 in COS-7 cells. As shown in **Figure 7b**, the triglyceride hydrolase activity of PNPLA2 was increased eightfold by CGI-58. Conversely, no lipase activity could be detected for PNPLA1, either

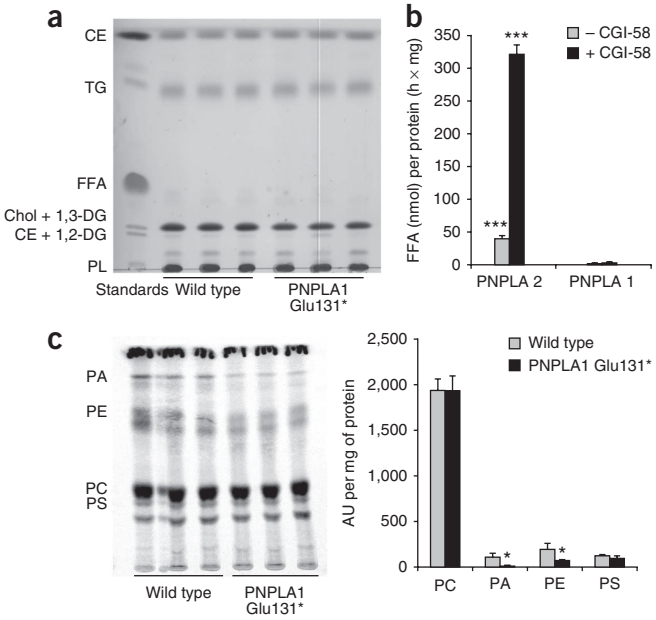

Figure 7 Triglyceride hydrolase activity and lipid profiles of wild-type and PNPLA1-deficient human keratinocytes in cell culture. (**a**) Neutral lipid profiles of wild-type and mutant human keratinocytes 7 d after induction of differentiation in culture. Lipids corresponding to 300 μg of protein were extracted and separated by thin-layer chromatography (TLC) using hexan/diethyl ether/glacial acetic acid (70:29:1) as solvent system. Spots were visualized by carbonization. (**b**) Triglyceride hydrolase activity of PNPLA1 and PNPLA2 in COS-7 cells transfected to express PNPLA1 and PNPLA2, with or without CGI-58, and measured by the release of radiolabeled fatty acids. β-galactosidase–transfected cells were used as the negative control and were set as the blank. (**c**) Incorporation of [^{14}C]-linoleic acid into phospholipids of differentiated wild-type and mutant human keratinocytes visualized after TLC by exposure to a phosphorimager screen and quantified with ImageQuant software. Data are presented as mean ± s.d. Statistical significance was determined by unpaired two-tailed Student's *t* test (*$P < 0.05$; ***$P < 0.001$). CE, cholesterol ester; TG, triglycerides; FFA, free fatty acids; Chol., cholesterol; DG, diglycerides; PL, phospholipids; PA, phosphatidic acid; PE, phosphatidylethanolamine; PC, phosphatidylcholine; PS, phosphatidylserine.

© 2012 Nature America, Inc. All rights reserved.

in the presence or absence of CGI-58. These results provide evidence that PNPLA1 does not have triglyceride hydrolase activity and is not influenced by CGI-58. Accordingly, an accumulation of lipid droplets was not observed in dog keratinocytes or leukocytes (Sudan black staining) or in the affected person's blood smear (data not shown). In addition, the vacuolic structures detected in the granular layer of affected dogs were not stained by oil red O (data not shown), indicating that they do not contain neutral lipids. To further investigate whether PNPLA1 affects phospholipid metabolism, we incubated differentiated wild-type and mutant keratinocytes with radiolabeled linoleic acid for 24 h. We found a substantial decrease in the incorporation of linoleic acid into phosphatidic acid and phosphatidylethanolamine species in mutant keratinocytes (**Fig. 7c**). Conversely, the incorporation into phosphatidylcholine and phosphatidylserine was unchanged. Together, this concordant series of experiments indicates that PNPLA1 has a role in glycerophospholipid rather than neutral lipid metabolism.

DISCUSSION

Ichthyosis in the golden retriever has recently spread throughout the breed because of the repeated use of champions and inbred crosses with affected or carrier dogs. Since the vital prognosis was not engaged, the disease has not been counter-selected and has thus rapidly spread throughout the breed with the frequency of the mutation now reaching 50%. Indeed, apart from desquamation, neither clinical nor biochemical or hematological abnormalities have been observed, which is concordant with the nonsystemic nature of the disease. Through a GWAS in this dog breed, followed by candidate gene sequencing, we identified a causative mutation in *PNPLA1*, which was not previously known to be involved in any form of ichthyoses or any other disease. Based on this discovery, we screened this gene in humans affected with ARCI and for whom no molecular cause had been identified. We identified two families carrying distinct mutations in the conserved catalytic patatin domain of *PNPLA1* gene, thus altering the functional role of the protein (**Fig. 2**). The causality of these mutations in humans is supported by a perfect segregation in an autosomal recessive mode of transmission. In addition, the fact that all affected individuals were collodion babies shows that the impairment is congenital and severe at birth. This clinical severity correlates well with the location of the mutations in the catalytic domain and with a major and specific role of PNPLA1 in the cutaneous barrier.

Here we provide the first evidence for the involvement of PNPLA1 in ichthyosis in dogs and humans. The human p.Glu131* mutation results in the loss of approximately half of the catalytic patatin domain, suggesting a complete loss of PNPLA1 function. Accordingly, no protein could be detected in the affected individual's keratinocyte cells by protein blotting experiments (**Fig. 6a**). In golden retriever dogs, the consequence of the mutation is the truncation of 74 amino acids from the C-terminal region of the protein. As the C-terminal part of PNPLA2 is considered to be the putative lipid binding site[8,9], we hypothesize that the *PNPLA1* indel has consequences for protein activity or localization and would also lead to a nonfunctional protein.

In addition to discovering a new gene causing ARCI, we provide evidence for the localization and function of PNPLA1 in the cutaneous barrier. First, dog *PNPLA1* mRNA expression is mostly detected in skin, and, specifically, in keratinocytes (**Supplementary Fig. 4a**). This observation is in agreement with the overexpression of the *PNPLA1* transcript in keratinocytes from the granular layer of the epidermis identified through the ORESTES method[44]. Immunolocalizations carried out on healthy human skin showed that PNPLA1 is expressed in the upper epidermis, predominantly in cells of the granular layer (**Fig. 4a–c**). Whereas PNPLA1 protein is clearly distributed in the cytoplasm of keratinocytes, immunoelectron microscopy experiments allowed refinement of its localization to the region of keratin filament bundles. However, contrary to other types of lipases[41,45], PNPLA1 does not localize to lamellar bodies, suggesting a pathogenic mechanism not linked to lipid transport via lamellar bodies (**Fig. 4d–f**). These results allow us to speculate that PNPLA1 activity takes place in the cytoplasm and is associated with the cytoskeleton. The expression of PNPLA1 is induced during *in vitro* keratinocyte differentiation. However, our observations suggest that lack of PNPLA1 does not directly affect the early stage of the differentiation process, as assessed by involucrin, but affects, at later stages, lamellar body function or formation as shown by CGI-58 protein reduction of expression (**Fig. 6b**).

Further insights into the pathogenic mechanisms of PNPLA1 in ichthyosis were provided by light and electron microscopy observations of similar ultrastructural features in affected golden retriever dogs and one human subject. These studies showed the presence of remnants of cholesterol crystals, which are structures typically associated with transglutaminase 1 (*TGM1*) deficiency[46], and irregular accumulations of abnormal membranous and vesicular material in keratinocytes of the granular layer that look like the consequence of a degenerative process in the intracellular membrane trafficking system (**Fig. 5**). Similar membrane structures, at the same intracellular location but with different ultrastructure, are also associated with *FATP4* mutations in ichthyosis prematurity syndrome[47]. Moreover, Ziblat *et al.*[48] reported cholesterol crystal nucleation and formation caused by artificially changing the composition of membrane lipids. Oil red O staining of frozen sections of dog skin showed that, as expected, the cornified layer was strongly colored in affected dogs and to a lesser extent in healthy dogs, but the perinuclear vacuolic regions of keratinocytes visible in affected dogs were not stained, indicating that these regions are not a site of neutral lipid accumulation. Concordant with the present results, Mauldin *et al.*[37] observed that keratinocytes of ichthyosis-affected golden retriever dogs contained "wispy granular material vacuoles." Indeed, these abnormal membrane structures are thought to be the consequence of PNPLA1 mutants causing lipid defects that could first lead to substantial disturbance of membrane organization and subsequently affect membrane trafficking processes as well as the entire endocytotic pathway.

PNPLA1 belongs to the patatin-like phospholipase family, for which associated diseases and/or functions have been described for all members except PNPLA1 (refs. 12,14,15). Although the *PNPLA1* gene was localized in the dog and human genome assemblies, its functional annotation as a lipid hydrolase was only putative (Swiss-Prot accession Q8N8W4). PNPLA1 to PNPLA5 are closely related proteins and could possess lipolytic and/or lipogenic properties, such as triglyceride lipase, hydrolase or transacetylase activities[14,15,49,50]. In contrast to PNPLA2, the PNPLA1 protein did not exhibit triglyceride lipase activity in the presence or absence of CGI-58, suggesting that these two proteins exhibit different substrate preferences (**Fig. 7**). Altogether, these results exclude PNPLA1 involvement in the neutral lipid metabolism of the skin, but they do indicate a role in the glycerophospholipid synthesis or remodeling, which could be mediated by acyl-CoA dependent or independent acyltransferase activity, as shown for PNPLA3 (ref. 14) and PNPLA4 (ref. 50).

In summary, we provide evidence for a key role of PNPLA1 in the lipid organization and metabolism of the epidermal barrier that is of prime importance in the keratinization process and terminal differentiation. The involvement for the first time of a PNPLA family gene

© 2012 Nature America, Inc. All rights reserved.

in ARCI provides a new link between this gene family and ichthyoses. Finally, the identification of the *PNPLA1* mutation using only a small number of case and control dogs is very promising for the discovery of other new human ichthyosis genes, given the segregation of different ichthyoses in several other dog breeds.

URLs. Human Protein Atlas, http://www.proteinatlas.org/; Cani-DNA Cani-DNA French Biobank of canine samples, http://dog-genetics.genouest.org/.

METHODS

Methods and any associated references are available in the online version of the paper at http://www.nature.com/naturegenetics/.

Accession codes. The dog and human *PNPLA1* cDNA reference sequences are available from GenBank under accession codes XM_538884.3 and NM_173676.2, respectively.

Note: Supplementary information is available on the Nature Genetics website.

ACKNOWLEDGMENTS

We thank A.S. Lequarré, an excellent coordinator for the European FP7 LUPA project, A. Boland and D. Zelenika for the genotyping performed at CNG (Evry, France); dermatologists, especially F. Caux, and Généthon, for patient DNA processing; J. Abadie (AMaROC research unit, Oniris, Ecole Nationale Vétérinaire de Nantes, France) and practitioners T. Bord, X. Langon, P. Prelaud, M.D. Vaillant, A. Muller and other veterinarians for providing us with clinical data and samples, as well as dog owners and breeders, especially J. Robidou, B. Facq, V. d'Alcantara and C. de Vinck. We thank P. Roosje and T. Leeb (University of Bern, Switzerland) for providing six Swiss golden retriever samples. We thank A. Fautrel and P. Bellaud, from the histopathology platform H^2P^2, IFR140 Biogenouest, (Rennes, France), M.D. Vignon-Pennamen from the anatomopathology laboratory of Saint Louis Hospital (Paris, France) and M. Werner from the Institute of Pathology at the University Hospital of Freiburg (Freiburg, Germany) who kindly provided paraffin human skin sections, as well as the Vébiotel laboratory (Arcueil, France) for dog sample biochemical analyses. We are grateful to G. Queney (Antagene, Lyon, France) and P. Quignon, G. Rabut and E. Watrin (Institut de Génétique et Développement de Rennes, France) for helpful discussions. Finally, we warmly thank S. Cure from Genoscope (Evry, France) for her several careful readings and English corrections and her kind availability, as well as D. Morris-Rosendahl (Institute for Human Genetics, Freiburg, Germany). This study was supported by CNRS, the European Commission (FP7-LUPA, GA-201370). R. Zechner and R. Zimmermann were supported by the FWF F30 SFB Lipotox, Z136 Wittgenstein, the GEN-AU project GOLD by the Austrian Ministry of Science and Research and FFG. I.H. was supported by the NIRK Network (German BMBF 01GM0904).

AUTHOR CONTRIBUTIONS

C.A., E.G. and F.G. designed the genetic aspects of the dog experiments. A.G., S.P., C.H., M.L.G., L.L. and S.K. performed the genetic and functional experiments for the dog studies. J. Fischer designed the human genetic analyses and supervised the functional studies on humans. E. Bourrat provided patient material and data. C.D. and G.-J.K. performed the genetic and microscopy experiments for the human studies. I.H. performed light and electron microscopy as well as immunoelectron microscopy investigations. F.D.-R. did H&E staining for histological diagnosis and investigations in dogs. S.G., F.P.W.R., R. Zimmermann and R. Zechner performed functional studies E.G., E. Bensignor, J. Fontaine and D.P., veterinarians specializing in dermatology, collected dog samples and interpreted clinical and biological data. A.T. provided 400 dog DNA samples and performed validation of the mutation in dogs. C.A., A.G., J. Fischer, F.G., C.H., M.L. and I.H.. contributed to the writing of the manuscript.

COMPETING FINANCIAL INTERESTS

The authors declare competing financial interests: details accompany the full-text HTML version of the paper at http://www.nature.com/naturegenetics/.

Published online at http://www.nature.com/naturegenetics/.
Reprints and permissions information is available online at http://www.nature.com/reprints/index.html.

1. Oji, V. *et al.* Revised nomenclature and classification of inherited ichthyoses: results of the First Ichthyosis Consensus Conference in Soreze 2009. *J. Am. Acad. Dermatol.* **63**, 607–641 (2010).
2. Fischer, J. Autosomal recessive congenital ichthyosis. *J. Invest. Dermatol.* **129**, 1319–1321 (2009).
3. Israeli, S. *et al.* A mutation in *LIPN*, encoding epidermal lipase N, causes a late-onset form of autosomal-recessive congenital ichthyosis. *Am. J. Hum. Genet.* **88**, 482–487 (2011).
4. Lefèvre, C. *et al.* Mutations in *CGI-58*, the gene encoding a new protein of the esterase/lipase/thioesterase subfamily, in Chanarin-Dorfman syndrome. *Am. J. Hum. Genet.* **69**, 1002–1012 (2001).
5. Demerjian, M., Crumrine, D.A., Milstone, L.M., Williams, M.L. & Elias, P.M. Barrier dysfunction and pathogenesis of neutral lipid storage disease with ichthyosis (Chanarin-Dorfman syndrome). *J. Invest. Dermatol.* **126**, 2032–2038 (2006).
6. Yamaguchi, T. & Osumi, T. Chanarin-Dorfman syndrome: deficiency in CGI-58, a lipid droplet-bound coactivator of lipase. *Biochim. Biophys. Acta* **1791**, 519–523 (2009).
7. Zimmermann, R., Lass, A., Haemmerle, G. & Zechner, R. Fate of fat: the role of adipose triglyceride lipase in lipolysis. *Biochim. Biophys. Acta* **1791**, 494–500 (2009).
8. Schweiger, M. *et al.* The C-terminal region of human adipose triglyceride lipase affects enzyme activity and lipid droplet binding. *J. Biol. Chem.* **283**, 17211–17220 (2008).
9. Fischer, J. *et al.* The gene encoding adipose triglyceride lipase (PNPLA2) is mutated in neutral lipid storage disease with myopathy. *Nat. Genet.* **39**, 28–30 (2007).
10. Ohkuma, A. *et al.* Distal lipid storage myopathy due to *PNPLA2* mutation. *Neuromuscul. Disord.* **18**, 671–674 (2008).
11. Akiyama, M. *et al.* Novel duplication mutation in the patatin domain of adipose triglyceride lipase (PNPLA2) in neutral lipid storage disease with severe myopathy. *Muscle Nerve* **36**, 856–859 (2007).
12. Lake, A.C. *et al.* Expression, regulation, and triglyceride hydrolase activity of Adiponutrin family members. *J. Lipid Res.* **46**, 2477–2487 (2005).
13. Wilson, P.A., Gardner, S.D., Lambie, N.M., Commans, S.A. & Crowther, D.J. Characterization of the human patatin-like phospholipase family. *J. Lipid Res.* **47**, 1940–1949 (2006).
14. Kienesberger, P.C., Oberer, M., Lass, A. & Zechner, R. Mammalian patatin domain containing proteins: a family with diverse lipolytic activities involved in multiple biological functions. *J. Lipid Res.* **50** (suppl.), S63–S68 (2009).
15. Baulande, S. & Langlois, C. Proteins sharing PNPLA domain, a new family of enzymes regulating lipid metabolism. *Med. Sci. (Paris)* **26**, 177–184 (2010).
16. Romeo, S. *et al.* Genetic variation in *PNPLA3* confers susceptibility to nonalcoholic fatty liver disease. *Nat. Genet.* **40**, 1461–1465 (2008).
17. Tian, C., Stokowski, R.P., Kershenobich, D., Ballinger, D.G. & Hinds, D.A. Variant in *PNPLA3* is associated with alcoholic liver disease. *Nat. Genet.* **42**, 21–23 (2010).
18. Rainier, S. *et al.* Neuropathy target esterase gene mutations cause motor neuron disease. *Am. J. Hum. Genet.* **82**, 780–785 (2008).
19. Mubaidin, A. *et al.* Karak syndrome: a novel degenerative disorder of the basal ganglia and cerebellum. *J. Med. Genet.* **40**, 543–546 (2003).
20. Tan, E.K., Ho, P., Tan, L., Prakash, K.M. & Zhao, Y. *PLA2G6* mutations and Parkinson's disease. *Ann. Neurol.* **67**, 148 (2010).
21. Gregory, A. *et al.* Neurodegeneration associated with genetic defects in phospholipase A(2). *Neurology* **71**, 1402–1409 (2008).
22. Sutter, N.B. & Ostrander, E.A. Dog star rising: the canine genetic system. *Nat. Rev. Genet.* **5**, 900–910 (2004).
23. Karlsson, E.K. *et al.* Efficient mapping of mendelian traits in dogs through genome-wide association. *Nat. Genet.* **39**, 1321–1328 (2007).
24. Galibert, F. & Andre, C. The dog: a powerful model for studying genotype-phenotype relationships. *Comp. Biochem. Physiol. Part D Genomics Proteomics* **3**, 67–77 (2008).
25. Cadieu, E. *et al.* Coat variation in the domestic dog is governed by variants in three genes. *Science* **326**, 150–153 (2009).
26. Parker, H.G. *et al.* An expressed *fgf4* retrogene is associated with breed-defining chondrodysplasia in domestic dogs. *Science* **325**, 995–998 (2009).
27. Merveille, A.C. *et al.* CCDC39 is required for assembly of inner dynein arms and the dynein regulatory complex and for normal ciliary motility in humans and dogs. *Nat. Genet.* **43**, 72–78 (2011).
28. Credille, K.M., Barnhart, K.F., Minor, J.S. & Dunstan, R.W. Mild recessive epidermolytic hyperkeratosis associated with a novel keratin 10 donor splice-site mutation in a family of Norfolk terrier dogs. *Br. J. Dermatol.* **153**, 51–58 (2005).
29. Credille, K.M. *et al.* Transglutaminase 1-deficient recessive lamellar ichthyosis associated with a LINE-1 insertion in Jack Russell terrier dogs. *Br. J. Dermatol.* **161**, 265–272 (2009).
30. Akiyama, M. & Shimizu, H. An update on molecular aspects of the non-syndromic ichthyoses. *Exp. Dermatol.* **17**, 373–382 (2008).
31. Huber, M. *et al.* Mutations of keratinocyte transglutaminase in lamellar ichthyosis. *Science* **267**, 525–528 (1995).
32. Parmentier, L. *et al.* Autosomal recessive lamellar ichthyosis: identification of a new mutation in transglutaminase 1 and evidence for genetic heterogeneity. *Hum. Mol. Genet.* **4**, 1391–1395 (1995).
33. Russell, L.J. *et al.* Mutations in the gene for transglutaminase 1 in autosomal recessive lamellar ichthyosis. *Nat. Genet.* **9**, 279–283 (1995).

© 2012 Nature America, Inc. All rights reserved.

34. Mauldin, E.A., Credille, K.M., Dunstan, R.W. & Casal, M.L. Clinical, histopathological and ultrastructural analysis of golden retriever ichthyosis. *Vet. Dermatol.* **18**, 187 (2007).
35. Guaguere, E., Bensignor, E., Muller, A., Degorce-Rubiales, F. & Andre, C. Epidemiological, clinical, histopathological and ultrastructural aspects of ichthyosis in golden retrievers: a report of 50 cases. *Vet. Dermatol.* **18**, 382–383 (2007).
36. Cadiergues, M.C. *et al.* Cornification defect in the golden retriever: clinical, histopathological, ultrastructural and genetic characterisation. *Vet. Dermatol.* **19**, 120–129 (2008).
37. Mauldin, E.A., Credille, K.M., Dunstan, R.W. & Casal, M.L. The clinical and morphologic features of nonepidermolytic ichthyosis in the golden retriever. *Vet. Pathol.* **45**, 174–180 (2008).
38. Guaguere, E. *et al.* Clinical, histopathological and genetic data of ichthyosis in the golden retriever: a prospective study. *J. Small Anim. Pract.* **50**, 227–235 (2009).
39. Purcell, S. *et al.* PLINK: a tool set for whole-genome association and population-based linkage analyses. *Am. J. Hum. Genet.* **81**, 559–575 (2007).
40. Adzhubei, I.A. *et al.* A method and server for predicting damaging missense mutations. *Nat. Methods* **7**, 248–249 (2010).
41. Akiyama, M. *et al.* CGI-58 is an alpha/beta-hydrolase within lipid transporting lamellar granules of differentiated keratinocytes. *Am. J. Pathol.* **173**, 1349–1360 (2008).
42. Eckert, R.L. *et al.* Regulation of involucrin gene expression. *J. Invest. Dermatol.* **123**, 13–22 (2004).
43. Hitomi, K. Transglutaminases in skin epidermis. *Eur. J. Dermatol.* **15**, 313–319 (2005).
44. Toulza, E. *et al.* Large-scale identification of human genes implicated in epidermal barrier function. *Genome Biol.* **8**, R107 (2007).
45. Elias, P.M., Williams, M.L., Holleran, W.M., Jiang, Y.J. & Schmuth, M. Pathogenesis of permeability barrier abnormalities in the ichthyoses: inherited disorders of lipid metabolism. *J. Lipid Res.* **49**, 697–714 (2008).
46. Laiho, E. *et al.* Clinical and morphological correlations for transglutaminase 1 gene mutations in autosomal recessive congenital ichthyosis. *Eur. J. Hum. Genet.* **7**, 625–632 (1999).
47. Klar, J. *et al.* Mutations in the fatty acid transport protein 4 gene cause the ichthyosis prematurity syndrome. *Am. J. Hum. Genet.* **85**, 248–253 (2009).
48. Ziblat, R., Leiserowitz, L. & Addadi, L. Crystalline domain structure and cholesterol crystal nucleation in single hydrated DPPC:cholesterol:POPC bilayers. *J. Am. Chem. Soc.* **132**, 9920–9927 (2010).
49. Johansson, L.E. *et al.* Genetic variance in the adiponutrin gene family and childhood obesity. *PLoS ONE* **4**, e5327 (2009).
50. Gao, J.G., Shih, A., Gruber, R., Schmuth, M. & Simon, M. GS2 as a retinol transacylase and as a catalytic dyad independent regulator of retinylester accretion. *Mol. Genet. Metab.* **96**, 253–260 (2009).

© 2012 Nature America, Inc. All rights reserved.

ONLINE METHODS

Sampling, genotyping and identification of the *PNPLA1* mutation in dogs. Blood and tissue biopsy samples from dogs were collected in Europe through the Cani-DNA Biobank (see URLs) by the network of veterinarians. The work with dog samples was approved by the CNRS ethical board, France (35-238-13) for UMR6061. Genomic DNA and RNA were extracted from blood and tissue samples, using the NucleoSpin® Blood L kit and the NucleoSpin® RNA II kit (Macherey-Nagel), respectively, according to the manufacturer's instructions. All affected golden retriever dogs had a histopathology diagnosis as described[38], and all the controls were over three years old with no scaling. Genotyping of 20 affected and 20 control dogs with the Affymetrix v2 canine SNP array was performed at the Centre National de Génotypage (CNG; Evry, France). Genotypes were analyzed and statistical *P* values calculated using PLINK software[39]. Mutation screening was performed on 12 affected and 12 unaffected dogs by Sanger sequencing of PCR product spanning the *PNPLA1* exons and exon/intron boundaries. Primers are listed in **Supplementary Table 2**. The presence or absence of the mutation was validated on 320 golden retrievers (120 affected and 200 unaffected), 180 healthy dogs belonging to other retriever breeds (curly coated retriever, flat coated retriever, Labrador retriever, Nova Scotia duck tolling retriever) and 300 healthy dogs from 25 other breeds among the 10 FCI (Fédération Cynologique Internationale) groups.

Human mutation screening. Blood samples from individuals with ARCI and their related family members were collected in collaboration with clinicians and the support of Généthon (Evry, France). DNA was extracted from whole blood using standard procedures. Informed consent was obtained from all subjects (affected individuals and their family members). The institutional committee of AFM/Généthon approved the study, conducted in accordance with the Declaration of Helsinki Principles. Genome-wide genotyping was carried out in consanguineous families (homozygosity mapping) using a panel of 400 microsatellite markers and the human SNP array (Illumina 370K). Ten families with homozygous regions around the *PNPLA1* gene were selected and all available members were sequenced for mutation screening. Primers for *PNPLA1* flanking the coding exons were designed with primer3 (**Supplementary Table 3**). Both strands from all subjects and controls were sequenced for the entire coding region and the exon/intron boundaries using standard protocols.

Dog *PNPLA1* cDNA analysis and RT-qPCR. Reverse transcription was performed on 1 μg of total RNA using the High-capacity cDNA Reverse Transcription kit (Applied Biosystems) according to the manufacturer's instructions. The total skin cDNA of the dog *PNPLA1* gene was amplified and sequenced using five primer pairs (listed in **Supplementary Table 4**). Expression analyses were carried out on 21 tissues as well as keratinocyte and fibroblast cells from healthy dogs. Those cell types were obtained by cell culture of a healthy dog skin biopsy. Cells were grown in DMEM GlutaMAX™ medium (Gibco BRL, Invitrogen) supplemented with 20% fetal bovine serum (FBS; PAA cell culture company) and 5% penicillin-streptomycin antibiotics (Gibco BRL, Invitrogen). Keratinocyte and fibroblast cells were separately cultivated at 37 °C in a controlled atmosphere with 5% CO_2. RT-qPCR was performed on 1:40 diluted cDNA samples with the SYBR Green PCR master mix (Applied Biosystems) on the 7900HT Fast Real-Time PCR System (Applied Biosystems) using standard procedures. Each PCR was carried out in triplicate. Relative amounts of the transcript were determined using the delta-delta Ct method. *GAPDH* was used as the reference gene (ENSCAFG00000015077). For each genotype, results were normalized with one of the five samples. Sequencing primers are listed in **Supplementary Table 4**.

Keratinocyte cell culture. Keratinocyte cell cultures were established according to standard protocols from a skin biopsy of a female with a Glu131* mutation in the *PNPLA1* gene. Adult human epidermal control keratinocytes were purchased from Invitrogen. Cells were seeded into 25-cm^2 flasks for protein blotting analysis and into 6-well plates for lipid analysis in serum-free EpiLife keratinocyte growth medium (Invitrogen) containing 60 μM $CaCl_2$ and supplemented with human keratinocyte growth supplement (HKGS) (Invitrogen), 100 mg/ml penicillin/streptomycin and 250 ng/ml amphotericin B, and were grown to 90–100% confluence. Keratinocyte differentiation was induced as described[51]. The medium was supplemented with 1.1 mM $CaCl_2$ and 10 μM linoleic acid complexed to BSA (ratio 3:1) for 7 days with medium changes every day.

Protein blotting analyses. Human wild-type and mutant keratinocytes were grown to confluence in serum-free growth medium with 60 μM $CaCl_2$ and then switched to growth medium supplemented with 1.1 mM $CaCl_2$ and 10 μM linoleic acid to induce differentiation. Cells were collected on day 0, day 3 and day 7 after differentiation induction in RIPA buffer (150 mM NaCl, 10 mM Tris-HCl, pH 7.4, 0.1% SDS, 1% Triton X-100, 1% sodium deoxycholate and 5 mM EDTA) and were lysed by sonication (Misonix Ultrasonic Liquid Processor, Misonix). After centrifugation at 1000*g* for 5 min to pellet nuclei and unbroken cells, the protein content was measured using BCA reagent (Pierce) with BSA as a standard. Twenty μg of protein was separated by 10% SDS-PAGE according to standard protocols, blotted onto polyvinylidene fluoride membrane (Carl Roth GmbH) and hybridized with a mouse polyclonal antibody raised against human PNPLA1 (1:1000 dilution, H00285848-B01, Abnova), mouse monoclonal antibody raised against human involucrin (1:1000 dilution, ab68, Abcam), mouse monoclonal antibody raised against human CGI-58 (1:1000 dilution, H00051099-M01, Abnova), rabbit polyclonal antibody raised against human transglutaminase 1 (1:1000 dilution, ab27000, Abcam) or rabbit monoclonal antibody raised against human GAPDH (1:10000 dilution, 2118, Cell Signaling). Specifically bound immunoglobulins were detected in a second reaction using horseradish peroxidase–conjugated anti-mouse or anti-rabbit IgG antibodies (1:10000 dilution) and visualized by enhanced chemiluminescence detection (ECL, GE Healthcare).

Histopathology and staining analyses. Hematoxylin and eosin staining was carried out following standard procedures on formalin-fixed paraffin embedded (FFPE) sections of total skin biopsies of affected and control golden retriever dogs and humans. Oil red O stainings were done following standard procedures on frozen sections of total skin biopsies of golden retriever dogs.

Confocal microscopy. Immunostaining was performed on FFPE sections of specimens from healthy humans using the following commercial antibodies: goat polyclonal antibody to PNPLA1 (1:100 dilution, sc-49708, Santa Cruz) and rabbit polyclonal antibody to filaggrin (1:100 dilution, PRB-417P, Covance) as primary antibodies, DyLight 549 donkey antibody to goat (1:150 dilution, 705-505-147) and DyLight 488 donkey antibody to rabbit (1:150 dilution, 711-485-152,both from Jackson ImmunoResearch) as secondary antibodies. Confocal images were captured and analyzed with a Carl Zeiss LSM 510 META laser scanning confocal microscope.

Immunoelectron microscopy examination. Immunoelectron microscopy was performed as previously described[52]. Briefly, Tokyasu cryo-ultrasections were cut from normal skin biopsy blocks (ca. $1mm^3$) fixed in 2% formaldehyde/0.2% glutaraldehyde in PBS for 1h, transferred in 1% formaldehyde in PBS, cryoprotected in 2.3 M sucrose overnight, block mounted and frozen in liquid nitrogen and cut with a Leica UC6 cryo-ultramicrotome at −90 °C. Ribbon sections were picked up with a sucrose-methylcellulose droplet in a wire loop and put on 3-mm copper grids. For immunolabeling, sections on grids were incubated in washing solution (phosphate-buffered saline; PBS), PNPLA1 antibody (sc-49708, Santa Cruz, dilution 1:20 in PBS and blocking solution), washing solution (PBS), 10 nm labeled secondary antibody (rabbit-antigoat IgG-gold, Aurion), washed with PBS and then with distilled water. Positive control: labeling with anti-filaggrin. Negative control: replacement of primary antibody with blocking solution. Contrasting grids were floated for 5 min on 2% uranyl acetate, passed over drops (on ice) of uranyl acetate-methylcellulose, picked up in a wire loop and allowed to dry.

Electron microscopy examination. Human and dog skin biopsies were fixed in 2.5% glutaraldehyde in 0.1 M sodium cacodylate buffer, pH 7.4, for at least 2 h, washed overnight and post-fixed with 1% aqueous osmium tetroxide for 1 h at 4 °C. After dehydration by ethanol and propylene oxide, the samples were embedded in Glycidether 100 (formerly Epon). After polymerization, semi-thin sections (1 μm) and ultrathin sections (70 to 90 nm) were cut with a Leica Ultracut E ultramicrotome. Semi-thin sections, observed using light

© 2012 Nature America, Inc. All rights reserved.

doi:10.1038/ng.1056

microscopy, were stained with methylene blue. Ultrathin sections were picked up onto copper grids coated with pioloform, contrasted with uranyl acetate and lead citrate solutions and investigated with a Zeiss EM900 electron microscope.

cDNA cloning of recombinant His-tagged proteins. The sequence containing the complete open reading frame of mouse *Pnpla1* was amplified by PCR from mouse cDNA with Phusion High-Fidelity DNA Polymerase (Biozym). cDNA was prepared from skin mRNA using the SuperScript Reverse Transcriptase protocol (Invitrogen). For subsequent cloning strategies, primers were designed to create endonuclease cleavage sites (**Supplementary Table 5**). The PCR product was then ligated via compatible restriction sites into the eukaryotic expression vector pcDNA4/HisMax (Invitrogen). The cloning of *PNPLA2* and *CGI-58* cDNA was described previously[53]. A control pcDNA4/HisMax vector expressing β-galactosidase was provided by the manufacturer (Invitrogen).

Expression of recombinant proteins and preparation of cell extracts. Monkey embryonic kidney cells (COS-7, ATCC CRL-1651) were transfected using Metafectene (Biontex GmbH) as described[54]. For the preparation of cell extracts, cells were collected by scraping, washed three times withPBS and disrupted in buffer A (0.25 M sucrose, 1 mM EDTA, 1 mM dithiothreitol, 20 mg/ml leupetine, 2 mg/ml antipain, 1 mg/ml pepstatin (pH 7.0)) by sonication (Misonix Ultrasonic Liquid Processor.Nuclei and unbroken cells were removed by centrifugation for 5 min at 1,000*g* at 4 °C. The expression of the His-tagged proteins was detected with protein blotting analysis as previously described[54].

Assay for triglyceride hydrolase activity. Triglyceride hydrolase activity was measured using phospholipid-emulsified triolein substrate containing [9,10-^{3}H] triolein as tracer. Release of radiolabeled fatty acids was determined by liquid scintillation counting. For the determination of triglyceride hydrolase activity, lysates of cells overexpressing *PNPLA1* or *PNPLA2* (40 μg protein/assay in a volume of 100 μl of buffer A) were incubated with 100 μl of substrate in a water bath for 60 min at 37 °C. Assays were performed in the presence and absence of cell lysates containing CGI-58. Cells expressing β-galactosidase were used as a negative control. After centrifugation (15 min at 800*g*), the radioactivity in 1 ml of the upper phase was determined by liquid scintillation counting. Triglyceride substrate was prepared by emulsifying, through sonication, 330 mM triolein (40,000 cpm/nmol) and 45 mM phosphatidylcholine/phosphatidylinositol (molar ratio of 3:1) in 100 mM potassium phosphate buffer (pH 7.0) and 5% defatted BSA.

Lipid analysis. To extract total lipids from differentiated keratinocytes, the cells were extracted twice with chloroform/methanol/glacial acetic acid (66:33:1). Lipids were collected from the organic phase after the addition of 1/5 vol of water. To monitor incorporation of ^{14}C-labeled linoleic acid into phospholipids, differentiated keratinocytes were incubated with 10 μM linoleic acid ([1-^{14}C]-linoleic acid, 50 nCi/nmol) complexed to BSA. After 24 h, cells were washed with PBS, and lipids were extracted twice with hexane/isopropanol (3:2) containing 0.1% glacial acetic acid. Lipids were dried, reconstituted in chloroform and spotted onto a Silica Gel 60 plate (Merck). Neutral lipids were developed in hexane/diethylether/glacial acetic acid (70:29:1) as solvent system. Spots were visualized by carbonization after spraying the plates with 10% $CuSO_4$ (w/v) and 10% H_3PO_4 (v/v) and heating them to 120 °C for 30 min. Radioactively labeled phospholipids were developed in $CHCl_3$/methanol/aceton/diethylether/glacial acetic acid/H_2O (50:10:20:12:5) as the solvent system and spots were visualized by exposure to a PhosphorImager Screen (ApBiotech). The signals were quantified using ImageQuant Software (Molecular Dynamics). After lipid extraction, cells were solubilized in 0.3 N NaOH, 0.1% SDS for 10 h at 37 °C, and the protein content was measured using BCA reagent (Pierce) and BSA as a standard.

51. Breiden, B., Gallala, H., Doering, T. & Sandhoff, K. Optimization of submerged keratinocyte cultures for the synthesis of barrier ceramides. *Eur. J. Cell Biol.* **86**, 657–673 (2007).
52. Slot, J.W. & Geuze, H.J. Cryosectioning and immunolabeling. *Nat. Protoc.* **2**, 2480–2491 (2007).
53. Lass, A. *et al.* Adipose triglyceride lipase-mediated lipolysis of cellular fat stores is activated by CGI-58 and defective in Chanarin-Dorfman Syndrome. *Cell Metab.* **3**, 309–319 (2006).
54. Zimmermann, R. *et al.* Fat mobilization in adipose tissue is promoted by adipose triglyceride lipase. *Science* **306**, 1383–1386 (2004).

© 2012 Nature America, Inc. All rights reserved.